

# RSC Advances



This is an *Accepted Manuscript*, which has been through the Royal Society of Chemistry peer review process and has been accepted for publication.

*Accepted Manuscripts* are published online shortly after acceptance, before technical editing, formatting and proof reading. Using this free service, authors can make their results available to the community, in citable form, before we publish the edited article. This *Accepted Manuscript* will be replaced by the edited, formatted and paginated article as soon as this is available.

You can find more information about *Accepted Manuscripts* in the [Information for Authors](#).

Please note that technical editing may introduce minor changes to the text and/or graphics, which may alter content. The journal's standard [Terms & Conditions](#) and the [Ethical guidelines](#) still apply. In no event shall the Royal Society of Chemistry be held responsible for any errors or omissions in this *Accepted Manuscript* or any consequences arising from the use of any information it contains.

# Aggregate-based sub-CMC Solubilization of Hexadecane by Surfactants

Hua Zhong<sup>1,2,3\*</sup>, Lei Yang<sup>1,2</sup>, Guangming Zeng<sup>1,2</sup>, Mark L. Brusseau<sup>3</sup>, Yake Wang<sup>3</sup>,  
Yang Li<sup>4</sup>, Zhifeng Liu<sup>1,2</sup>, Xingzhong Yuan<sup>1,2</sup>, Fei Tan<sup>1,2</sup>

<sup>1</sup> College of Environmental Science and Engineering, Hunan University, Changsha  
410082, China;

<sup>2</sup> Key Laboratory of Environmental Biology and Pollution Control (Hunan  
University), Ministry of Education, Changsha, 410082, China;

<sup>3</sup> Department of Soil, Water and Environmental Science, University of Arizona,  
Tucson, Arizona 85721, U.S.A.;

<sup>4</sup> Department of Chemistry, University of Science and Technology of China, Hefei,  
230026, China.

Submitted to:

*RSC Advances*

26 June 2015

## Email Addresses:

Hua Zhong: zhonghua@email.arizona.edu

Lei Yang: wlwyanglei@126.com

Guangming Zeng: zgming@hnu.edu.cn

Mark L Brusseau: brusseau@email.arizona.edu

Yake Wang: yakew@email.arizona.edu

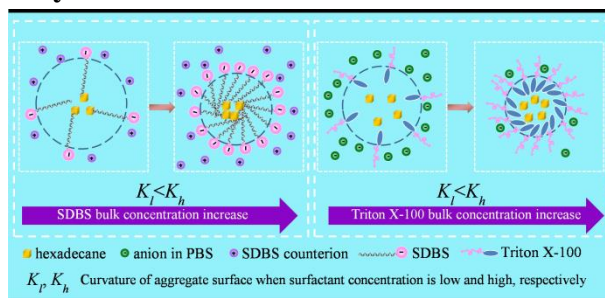
Yang Li: ly2013fi@mail.ustc.edu.cn

Zhifeng Liu: lzf18182002@163.com

Xingzhong Yuan: yxz@hnu.edu.cn

Fei Tan: tanfei\_2013@163.com

## Table of contents entry:



SDBS or Triton X-100 at sub-CMC concentrations enhances hexadecane solubilization due to aggregate formation mechanism. The sub-CMC aggregate size decreases with increasing surface excess of surfactant.

## 1 **Abstract**

2 Solubilization of hexadecane by two surfactants, SDBS and Triton X-100, at  
3 concentrations near the critical micelle concentration (CMC) and the related  
4 aggregation behavior was investigated in this study. Solubilization was observed at  
5 surfactant concentrations lower than CMC, and the apparent solubility of  
6 hexadecane increased linearly with surfactant concentration for both surfactants. The  
7 capacity of SDBS to solubilize hexadecane is stronger at concentrations below CMC  
8 than above CMC. In contrast, Triton X-100 shows no difference. The results of  
9 dynamic light scattering (DLS) and cryogenic TEM analysis show aggregate  
10 formation at surfactant concentrations lower than CMC. DLS-based size of the  
11 aggregates ( $d$ ) decreases with increasing surfactant concentration. Zeta potential of  
12 the SDBS aggregates decreases with increasing SDBS concentration, whereas it  
13 increases for Triton X-100. The surface excess ( $\Gamma$ ) of SDBS calculated based on  
14 hexadecane solubility and aggregate size data increases rapidly with increasing bulk  
15 concentration, and then asymptotically approaches the maximum surface excess  
16 ( $\Gamma_{\max}$ ). Conversely, there is only a minor increase in  $\Gamma$  for Triton X-100. Comparison  
17 of  $\Gamma$  and  $d$  indicates that excess of surfactant molecules at aggregate surface has  
18 great impact on surface curvature. The results of this study demonstrate formation of  
19 aggregates at surfactant concentrations below CMC for hexadecane solubilization,  
20 and indicate the potential of employing low-concentration strategy for surfactant  
21 application such as remediation of HOC contaminated sites.

22 **Keywords:** surfactant, SDBS, Triton X-100, critical micelle concentration,  
23 solubilization, aggregation.

## 24 1. Introduction

25 Today surfactants have been a chemical that is ubiquitously used in industries  
26 and households. One well-known function of surfactants is to solubilize  
27 hydrophobic organic compounds (HOCs), which has been widely made use of,  
28 ranging from oily dirt removal from textiles for housekeeping to enhanced  
29 remediation of soil or aquifer contaminated by HOCs.<sup>1-3</sup> Solubilization enhancement  
30 of HOCs by surfactants has been the subject of many experimental and theoretical  
31 studies, especially at concentrations above CMCs.<sup>4-10</sup> Critical micelle concentration  
32 (CMC) is generally considered to be the concentration at which surfactant molecules  
33 aggregate to form micelles. Micelles are considered to be of spherical shape, and the  
34 size, shape, aggregation number, and stability of micelles vary according to  
35 temperature, surfactant concentration, and solution chemistry.<sup>11</sup> It is typically  
36 assumed that surfactants solubilize low-solubility compounds only at concentrations  
37 higher than CMC, through partitioning into the hydrophobic core of micelles.<sup>9, 12, 13</sup>

38 The results of some studies have shown, however, that solubilization  
39 enhancement may also occur at surfactant concentration below the CMC. Zhang and  
40 Miller<sup>6</sup> investigated solubilization of octadecane by rhamnolipid biosurfactant.  
41 Solubilization of octadecane was enhanced by rhamnolipid at concentrations below  
42 CMC, and the enhancement was much more significant than above CMC. Similar  
43 results were observed for hexadecane solubilization in the presence of a  
44 monorhamnolipid in our prior study.<sup>14</sup> Kile and Chlou investigated solubilization of

45 DDT by surfactant Triton and Brij, and enhancement of apparent DDT solubility  
46 was also observed below the nominal CMC.<sup>5</sup> To our knowledge, the mechanisms for  
47 these sub-CMC solubilization behaviors, for example the potential for aggregate  
48 formation below CMC, have not been systematically investigated in prior studies.  
49 Moreover, concerns about the ecotoxicology of surfactants, e.g. alkylphenol  
50 ethoxylates (APEs)<sup>15, 16</sup>, has caused the implementation of strict emission controls  
51 for APEs in various industrial and consumer applications.<sup>17-20</sup> Thus, the ability for  
52 surfactants to achieve solubilization enhancement of HOCs at sub-CMC  
53 concentrations is of importance for cost and ecotoxicology considerations.

54 In this study, solubilization of *n*-hexadecane in the presence of SDBS or Triton  
55 X-100 surfactant was investigated, with a special focus on such behavior at  
56 surfactant concentrations below CMC. SDBS and Trion X-100 were selected to  
57 represent anionic and nonionic surfactant, respectively. In addition to hexadecane  
58 solubility, characterizations of the potential aggregation of the surfactants, such as  
59 aggregate particle size and zeta potential measurements and cryo-TEM-based  
60 aggregate observation, were implemented. Finally, based on surfactant interface  
61 adsorption theory, spherical aggregate assumption and surfactant mass balance, the  
62 aggregation formation and surfactant partitioning mechanism was raised to interpret  
63 the sub-CMC hydrocarbon solubilization.

64

## 65 2. Theoretical



66 At a given temperature, adsorption of surfactant to the hexadecane/aqueous  
67 solution interface is related to interfacial tension and surfactant bulk activity as  
68 expressed by the Gibbs adsorption equation.<sup>21</sup> In this study, the adsorption of ionic  
69 and nonionic surfactant at the interface in the presence of swamping counterion  
70 (electrolyte solution) can be described by equation (1):

$$71 \quad \Gamma = -\frac{a}{RT} \left( \frac{d\gamma}{da} \right) \times 10^{-3} \quad (1)$$

72 where  $a$  is the surfactant bulk activity (mol/L);  $R$  is the universal gas constant  
73 (8.314 J/(mol K)),  $T$  (K) is the absolute temperature;  $\Gamma$  (mol/m<sup>2</sup>) is the interface  
74 excess of the surfactant;  $\gamma$  (mN/m) is the interfacial tension.

75 Surfactant adsorption at fluid-fluid interfaces is described by the Langmuir  
76 equation at concentrations below the critical micelle concentration (CMC)<sup>8, 22</sup>:

$$77 \quad \Gamma = \Gamma_{\max} \frac{Ka}{1+Ka} \quad (2)$$

78 where  $\Gamma_{\max}$  (mol/m<sup>2</sup>) is the maximum interface excess of surfactant and  $K$  (L/mol)  
79 is the Langmuir constant.

80 Resolving equation (1) and combining it with equation (2) give the  
81 Szyszkowski equation, which describes interfacial tension as a function of surfactant  
82 bulk activity at concentrations below CMC:

$$83 \quad \gamma_0 - \gamma = RT\Gamma_{\max} \ln(1 + Ka) \times 10^3 \quad (3)$$

84 where  $\gamma_0$  (mN/m) is the interfacial tension of the solution in the absence of surfactant.  
85 The relation between  $a$  and the freely-dissolved surfactant monomer concentration,  
86  $C_w$  (mol/L), is:

$$87 \quad a = fC_w \quad (4)$$

88 where  $f$  is the activity coefficient of surfactant. The concentration of surfactants in  
 89 bulk solution is relatively low ( $<0.01$  mol/L) in this study, thus  $f$  is very close to 1  
 90 and  $a \approx C_w$ .<sup>22</sup>

91 Based on the classical model regarding the structure of alkane-surfactant  
 92 aggregates formed in solution for alkane solubilization, the aggregates are assumed  
 93 to be spherical with a layer of surfactant molecules on the surface. Thus, when  
 94 solubilization reaches equilibrium, equation (5) and (6) can be obtained based on  
 95 mass balance of surfactant:

$$96 \quad \frac{\Gamma A_i C_{\text{hex}} M_{\text{hex}}}{\rho_{\text{hex}}} \times 10^{-3} + C_w = C_0 \quad (5)$$

$$97 \quad A_i = \frac{6}{d} \times 10^{-9} \quad (6)$$

98 where  $A_i$  ( $\text{m}^2/\text{m}^3$ ) is the hexadecane-water specific interfacial area;  $C_0$  (mol/L) is the  
 99 total concentration of surfactant initially added;  $C_{\text{hex}}$  (mol/L) is the concentration of  
 100 hexadecane solubilized in aqueous phase;  $M_{\text{hex}}$  (g/mol) is molecular weight of the  
 101 hexadecane; and  $\rho_{\text{hex}}$  ( $\text{g}/\text{cm}^3$ ) is the density of the hexadecane at given temperature  
 102  $T$  (K);  $d$  (nm) is the measured diameter of the aggregates. From equation (3), (4), (5)  
 103 and (6), the surfactant excess,  $\Gamma$ , of surfactant on the aggregate surface and the  $C_w$   
 104 for a given  $C_0$  can be obtained. The area per surfactant molecule at the  
 105 hexadecane-aqueous interface (namely the aggregate surface),  $A$  ( $\text{m}^2$ ), is obtained by  
 106 equation (7):

$$107 \quad A = \frac{1}{\Gamma N_A} \quad (7)$$

108 where  $N_A(6.022 \times 10^{23} \text{ mol}^{-1})$  is the Avogadro constant.

109

### 110 **3. Materials and methods**

#### 111 **3.1 Materials**

112 SDBS (Sodium dodecylbenzenesulfonate, technical grade, purity > 97.0%),  
113 Triton X-100 (polyoxyethylene (10) isooctylphenyl ether, laboratory grade, purity >  
114 98.0%), and hexadecane (purity > 99.0%) were purchased from Sigma-Aldrich (St.  
115 Louis, Mo., U.S.). Selected properties and molecular structures of SDBS and Triton  
116 X-100 are presented in Table 1 and Fig. 1, respectively. *n*-Octane (purity > 95.0%)  
117 and HPLC grade ethanol were purchased from Damao Chemical (Tianjin, China).  
118 All other chemicals were of analytical grade and used as received. Ultra-pure water  
119 with an initial resistivity of 18.2 M $\Omega$ ·cm produced by UPT- II -40 (Ulupure,  
120 Chengdu, China) was used throughout the experiment. Phosphate buffer solution  
121 (PBS, 1.24 g/L KH<sub>2</sub>PO<sub>4</sub> and 1.35 g/L K<sub>2</sub>HPO<sub>4</sub> · 3H<sub>2</sub>O, pH 6.8) was used as the  
122 background electrolyte solution to provide a stable concentration of counterions,  
123 which is important for application of the Gibbs adsorption equation for surfactant  
124 surface excess calculation.

125

#### 126 **3.2 Interfacial tension measurement**

127 In order to obtain the CMCs of the surfactants and  $\Gamma_{\max}$  and  $K$  in equation (3),  
128 interfacial tension between hexadecane and surfactant solution with designated

129 surfactant concentrations was measured at 30 °C with a tensiometer (JZ-200A,  
130 Chengde, China) using the Du Noüy Ring method.<sup>23</sup> In brief, 15 mL of surfactant  
131 PBS solution was prepared in a 50 mL glass beaker. 15 mL of hexadecane was then  
132 carefully added to the top of the surfactant solutions without disturbing the bulk  
133 volumes. Before the interfacial tension was measured, the beaker was kept at 30 °C  
134 for half an hour to allow partition of surfactant to water-hexadecane interface to  
135 reach equilibrium. The measurements were reproducible, with the difference of  
136 duplicate measurements within  $\pm 0.2$  mN/m.

137

### 138 **3.3 Solubilization of hexadecane by surfactants**

139 Solutions of SDBS and Triton X-100 with hexadecane were prepared in  
140 triplicates using the following procedures. 50  $\mu$ L of hexadecane was pipetted to a  
141 25-mL glass flask, and the flask was rotated to spread the hexadecane on the bottom  
142 of the flask. 10 mL of PBS solution of SDBS or Triton X-100 was then added to the  
143 flask and incubated on a reciprocal shaker at 30 °C, 120 rpm for 72 h to allow the  
144 solubilization to reach equilibrium (result of a preliminary test showed that  
145 hexadecane solubility does not change after 72 h). Then the flasks were held  
146 stationary for 2 h to allow establishment of stable phase distributions. 4 ml of the  
147 aqueous solution was separated and collected using the method described by Zhong  
148 et al.<sup>14</sup>. 1 mL of the collected samples was removed for hexadecane concentration  
149 measurement, and another 2 mL was used for measurement on size and zeta

150 potential of the aggregate particles. The hexadecane concentration was measured  
151 using gas chromatography (Agilent GC 6890N) following the procedures described  
152 by Zhong et al.<sup>14</sup>. Samples with 8000  $\mu\text{M}$  SDBS or with 1000  $\mu\text{M}$  Triton X-100  
153 were centrifugally filtered using 30KD ultrafiltration membrane (Millipore,  
154 Darmstadt, Germany) followed by hexadecane concentration measurement in the  
155 filtrate to check the partition of hexadecane. A control containing 10 mL surfactant  
156 solution and no hexadecane was used to quantify loss of surfactant due to adsorption  
157 to inner wall of the flasks. To examine the stability of solubilized hexadecane, 4 mL  
158 of the solubilized hexadecane solution obtained with 50  $\mu\text{M}$  SDBS or 25  $\mu\text{M}$  Triton  
159 X-100 were sealed and allowed to stand still for 48 hours. Then 3 mL of the solution  
160 were again centrifugally separated using the method described by Zhong et al.<sup>14</sup> and  
161 hexadecane concentration was measured.

162 The size and zeta potential of aggregate particles were measured using a  
163 ZEN3600 Zetasizer Nano (Malvern Instruments, U.K.). The particle size was  
164 determined through dynamic light scattering (DLS) at 633 nm with He-Ne laser,  
165 which worked on 4.0 mV power. 1 mL of sample was loaded to the DTS-0012 cell  
166 and kept at 30  $^{\circ}\text{C}$ . The scattered light was collected by receptor at angle of 173  $^{\circ}$  from  
167 light path. The size of the aggregates was expressed in terms of hydrodynamic  
168 diameter, which was calculated by using the software associated with the instrument.  
169 To obtain the zeta potential of the aggregates, approximately 1 mL of sample was  
170 loaded to the DTS1060 folded capillary cell and the electrophoretic mobility of the

171 aggregate particles was measured at 30 °C under automatic voltage using laser  
172 Doppler velocimetry with M3-PALS technique to avoid electrosmosis. The  
173 measured data was converted into corresponding zeta potential applying the  
174 Helmholtz-Smoluchowski equation.<sup>24</sup>

175

### 176 **3.4 Cryo-Transmission Electron Microscopy (cryo-TEM) observation of** 177 **aggregates**

178 A 4 µL drop of sample was placed on the copper grid, and then sent to a FEI  
179 Vitrobot sample plunger. The excess sample was removed with filter paper. The grid  
180 was then immediately plunged into a bath of liquid ethane and transferred to a bath  
181 of liquid nitrogen. The samples were stored in a GATAN model cryo-transfer unit in  
182 liquid nitrogen. The morphology of surfactant-hexadecane aggregates was viewed  
183 with a Tecnai F20 cryo-transmission electron microscope (FEI, Hillsboro, Oregon)  
184 at 120 kV.

185

## 186 **4. Results and discussion**

### 187 **4.1 $\Gamma_{max}$ and $K$**

188 The dependence of interfacial tension on the surfactant concentration is  
189 presented in Fig. 2a. The interfacial tension of hexadecane/PBS solution in the  
190 absence of surfactants is 41.3 mN/m. For SDBS, hexadecane/PBS interfacial tension  
191 decreases rapidly from 41.2 to 2.3 mN/m with increase of the SDBS concentration

192 to approximately 600  $\mu\text{M}$ . Further increase in SDBS concentration has minimal  
193 effect on the interfacial tension. For Triton X-100, the interfacial tension decreases  
194 from 41.3 to 4.2 mN/m with increase in the Triton X-100 concentration to  
195 approximately 500  $\mu\text{M}$ . Further increase in Triton X-100 concentration slowly  
196 reduces the interfacial tension from 4.2 to 1.4 mN/m.

197 CMCs of the surfactants were obtained using the method described by Zhong et  
198 al.<sup>25</sup>. The CMC of SDBS is 612  $\mu\text{M}$ , which is lower than in pure water (e.g. 2764  
199  $\mu\text{M}$  reported by Yang et al.<sup>26</sup>) due to the presence of counterions (i.e.,  $\text{K}^+$ ) in PBS in  
200 this study. The CMC of Triton X-100 is 672  $\mu\text{M}$ , which is in the range of 200-900  
201  $\mu\text{M}$  reported by Sigma-Aldrich.<sup>27</sup> The significantly different CMCs for PBS versus  
202 water obtained for SDBS compared to the similar values obtained for Triton is  
203 consistent with the anionic and nonionic natures of the two, respectively.

204 The interfacial tension data at surfactant concentrations below CMC were well  
205 fitted by the logarithmic function described by Equation (3) (Fig. 2b), and the  
206 maximum interface excess of surfactant ( $\Gamma_{\text{max}}$ ) and the Langmuir constant ( $K$ ) were  
207 thus obtained. Minimal surfactant molecule area at interface ( $A_m$ ) was calculated  
208 using equation (7). The results are summarized in Table 1.

209

#### 210 **4.2 Solubilization of hexadecane by surfactants**

211 As shown in Table S1, concentration of hexadecane solubilized by 50  $\mu\text{M}$   
212 SDBS or 25  $\mu\text{M}$  Triton X-100 after standing for 48 hours is essentially identical to

213 the initial concentration. 50  $\mu\text{M}$  and 25  $\mu\text{M}$  are lower end concentrations,  
214 respectively, for SDBS and Triton X-100 used in this study. The results demonstrate  
215 good stability of the solubilized hexadecane. Results of hexadecane solubilization by  
216 SDBS and Triton X-100 are presented in Fig. 3. Both surfactants increase the  
217 solubility of hexadecane at surfactant concentrations lower than CMC. The apparent  
218 solubility of hexadecane increased linearly with surfactant concentration for both  
219 surfactants, with different slopes below and above CMC. Solubilization capacity of a  
220 surfactant for an HOC is characterized by the molar solubilization ratio (MSR),  
221 which is defined as increase of solubilized hydrophobic compound concentration  
222 (mol/L) per unit increase of surfactant concentration (mol/L) in the solution.<sup>12, 28</sup> As  
223 shown from Fig. 3a, the MSR for SDBS is significantly higher below CMC than  
224 above CMC (i.e. 0.84 and 0.16, respectively). Similar results were observed for an  
225 ionic rhamnolipid biosurfactant in the solubilization of hexadecane<sup>14</sup> and  
226 octadecane<sup>6</sup>. In contrast, MSRs for Triton X-100 are not significantly different  
227 below and above CMC (1.9 and 1.5, Fig. 3b), indicating the influence of surfactant  
228 molecule structure on solubilization behavior.

229

### 230 **4.3 Size and zeta potential of aggregates**

231 Formation of aggregates at surfactant concentrations both below and above  
232 CMC is demonstrated by the results of aggregate size measurement using DLS  
233 method (Fig.4) and by direct view of the aggregates with cryo-TEM for Triton



234 X-100 at concentrations of 25 and 1500  $\mu\text{M}$  (Fig. S1, Supplementary Information).  
235 Also, the spherical aggregate assumption was confirmed by the sphere morphology  
236 of the aggregates. Although three groups of particles with different size range (three  
237 peaks in the intensity and volume of particles distributions (%) plots, Fig. S2) were  
238 detected by DLS particle size measurement, almost 100% of the particles in  
239 numbers are in the group of the smallest size (Figs. S2 and S3). This is consistent  
240 with the results of the cryo-TEM measurements, in which only one group of  
241 particles with similar size was observed (Fig. S1). For both surfactants, the particle  
242 size decreases rapidly with increase of  $C_0$  to approximately 200  $\mu\text{M}$ , and then  
243 stabilizes as  $C_0$  continues to increase to above CMC (Fig.4).

244 As shown in Fig. 5, for anionic surfactant SDBS, the zeta potential of  
245 aggregates decreases approximately from -20 mV to -35 mV with increase of  $C_0$   
246 from 25  $\mu\text{M}$  to 200  $\mu\text{M}$ , and stabilizes at  $\sim$  -35 mV with further increasing  $C_0$  to 800  
247  $\mu\text{M}$ . Similar trend was observed by Ivanov et al.<sup>29</sup> for zeta potential of hexadecane  
248 emulsion drops versus concentration of ionic surfactant SDS at significantly low  
249 SDS concentrations. When  $C_0$  is even further increased to 1200  $\mu\text{M}$ , a secondary  
250 decrease of zeta potential to  $\sim$ -70 mV is observed. In contrast, the zeta potential of  
251 hexadecane-Triton X-100 aggregates increased from -20 mV to -5 mV with  
252 increasing  $C_0$  from 50  $\mu\text{M}$  to 1000  $\mu\text{M}$  and stabilized at  $\sim$ -5 mV when  $C_0$  was above  
253 1000  $\mu\text{M}$ . Zeta potential is the potential difference between the bulk solution of the  
254 dispersion medium and the slippery layer of fluid attached to the dispersed

255 particle.<sup>24, 30</sup> Due to the anionic hydrophilic heads of SDBS, the aggregates have  
256 negatively charged surface.<sup>31</sup> The negatively charged surface of aggregates for  
257 non-ionic Triton X-100 probably results from association of anions in PBS (i.e. OH<sup>-</sup>,  
258 HPO<sub>4</sub><sup>2-</sup>, H<sub>2</sub>PO<sub>4</sub><sup>-</sup>, PO<sub>4</sub><sup>3-</sup>) with the polyoxyethylene chain of Triton on the aggregate  
259 surface.

260

#### 261 **4.4 Partitioning of surfactants and its relation with aggregation**

262 In the experiments no emulsion of hexadecane in the presence of surfactants  
263 was observed. Adsorption of the surfactants to the inner wall of the flask was also  
264 minimal (data not shown). Because very limited volume of hexadecane (50 µL) was  
265 used, partition of surfactants to the hexadecane phase, or to the interface between the  
266 floating mass of hexadecane and the aqueous phase (less than 1 cm<sup>2</sup> in contrast to  
267 the magnitude of 10<sup>2</sup>~10<sup>4</sup> cm<sup>2</sup> for the total surface area of the aggregates according  
268 to calculation below), was minimal. Therefore, the surfactants reside either in bulk  
269 aqueous solution or in the aggregate. The hexadecane concentration in the filtrate  
270 after ultrafiltration was under the detection limit (data not shown), showing that the  
271 amount of freely-dissolved hexadecane in bulk aqueous phase is minimal and all the  
272 solubilized hexadecane is associated with aggregate. This is consistent with the fact  
273 that hexadecane has extremely low water solubility (0.09 µg/L, 25 °C) and high  
274 octanol-water partition coefficient (10<sup>8.3</sup>, 25 °C) of hexadecane.<sup>32</sup> Hence, based on  
275 the spherical aggregate assumption, the aggregate surface excess  $\Gamma$  and the bulk

276 concentration  $C_w$  of surfactants were calculated by applying equation (2) and (5)  
277 using  $\Gamma_{\max}$  and  $K$  previously obtained.

278 For both SDBS and Triton X-100, a linear relationship between the apparent  
279 solubility of hexadecane,  $C_{\text{hex}}$ , and the freely-dissolved surfactant monomer  
280 concentration,  $C_w$ , is observed with increase of  $C_w$  to CMC (Fig. 6a). This is similar  
281 to the relationship between  $C_{\text{hex}}$  and the total surfactant concentration,  $C_0$  (Fig. 3).  
282 By comparing the slopes of  $C_{\text{hex}}-C_0$  profile at  $C_0$  below CMC and  $C_{\text{hex}}-C_w$  profile  
283 (0.84 versus 1.0 for SDBS, and 1.9 versus 2.5 for Triton X-100), the relative  
284 distribution of the surfactant between the freely-dissolved and aggregate-associated  
285 is calculated. The percentage of the aggregate-associated surfactant is approximately  
286 16% and 23% of the total for SDBS and Triton X-100, respectively.

287 Changes of surfactant surface excess ( $\Gamma$ ) and molecule area ( $A$ ) versus  $C_w$  are  
288 presented in Fig. 6b. For SDBS, a rapid increase of  $\Gamma$  and decrease of  $A$  are observed  
289 when  $C_w$  increases from  $\sim 25 \mu\text{M}$  to  $\sim 150 \mu\text{M}$ . Further increase of  $C_w$  causes  
290 asymptotic approach of  $\Gamma$  and  $A$  to  $\Gamma_{\max}$  and  $A_m$ , respectively. Conversely, there is  
291 only a minor increase in  $\Gamma$  for Triton X-100. Only very slight increase of  $\Gamma$  and  
292 decrease of  $A$  are observed when  $C_w$  was below  $\sim 80 \mu\text{M}$ .  $\Gamma$  and  $A$  are more  
293 sensitive to change of  $C_w$  with a smaller  $K$  according to equation (2) and (7). The  $K$   
294 value for Triton X-100 is much larger than for SDBS ( $4.33 \times 10^3$  and  $0.2 \times 10^3 \text{ m}^3/\text{mol}$ ,  
295 respectively (Table 1)). Thus, a more significant change of  $\Gamma$  and  $A$  over a broader  
296 range of  $C_w$  occurred for SDBS.

297 As shown in Fig. 7, for both surfactants, aggregate size,  $d$ , decreases with the  
298 increase of surfactant surface excess on the aggregates,  $\Gamma$ , in a way that  $d$  approaches  
299 the stabilized minimum aggregate size ( $d_{\min}$ ) as  $\Gamma$  approaches  $\Gamma_{\max}$ . This result  
300 indicates that the curvature of the aggregate surface increases with increasing  
301 surface density of surfactant molecules. For SDBS, which has charged hydrophilic  
302 head, as SDBS molecules approach each other ( $\Gamma$  increases and  $A$  decreases) on the  
303 aggregate surface, the electrostatic repulsion between charged heads of SDBS  
304 becomes stronger. Such enhancement in electrostatic repulsion induces unequal rate  
305 of approach for polar and hydrophobic moieties between molecules, and therefore  
306 increase in aggregate surface curvature (Fig. 8). Thus, the aggregate size,  $d$ ,  
307 decreases with increasing  $\Gamma$ . Similarly, as the polar head of Triton X-100 molecule,  
308 the polyoxyethylene chain, usually twists and curls, causing large actual molecule  
309 radius<sup>33</sup>, the spatial steric repulsion between Triton X-100 polar heads may act in a  
310 way similar to electrostatic repulsion between charged heads in SDBS molecules,  
311 thus also causing an increase in surface curvature of aggregates (Fig. 8).

312 Zeta potential is a function of particle size and surface charge density.<sup>24, 34, 35</sup>  
313 Because SDBS is an anionic surfactant with a polar head that fully dissociates in  
314 solution, surface charge density is determined by surface molecule density, or  $\Gamma$ .  
315 Also, as discussed above, particle size is also a function of  $\Gamma$ . For SDBS, therefore,  
316 zeta potential is essentially a dependent of  $\Gamma$  and its change also exhibits an  
317 asymptotic pattern at concentrations lower than CMC. For Triton X-100, binding of

318 anions, i.e.  $\text{H}_2\text{PO}_4^-$ ,  $\text{HPO}_4^{2-}$  and  $\text{OH}^-$ , to the polyoxyethylene group through  
319 hydrogen bond may be responsible for the negative zeta potential of the aggregates.  
320 As  $\Gamma$  increases, the Triton X-100 molecules become more compacted on the  
321 aggregate surface, leaving less space for the anions to partition. Consequently zeta  
322 potential increases.

323 For the standard surfactant solubilization conceptualization, enhancement of  
324 HOC solubility requires surfactant concentrations higher than CMC.<sup>28, 36-38</sup> In  
325 contrast, results in this study show that significant hexadecane solubility  
326 enhancement takes place at surfactant concentrations lower than CMC and such  
327 enhancement is related to formation of aggregates. In fact, the CMC measurement  
328 using the general methods, e.g. the interfacial tension and conductometric methods,  
329 is based on a pure-surfactant micelle formation mechanism. We speculate that the  
330 presence of hexadecane has some influence on surfactant monomers activity through  
331 the hydrophobic interaction between surfactant and hexadecane molecules, which  
332 may be more significant than between surfactant molecules themselves. Thus, the  
333 interaction between surfactant and hexadecane molecules may favor formation of  
334 aggregates in priority to formation of pure-surfactant micelles, leading to  
335 hexadecane solubilization enhancement below CMC.

336 When surfactant concentration in the aqueous phase is higher than CMC, the  
337 surfactant molecules form micelles. Co-existence of hexadecane-SDBS aggregates  
338 and SDBS micelles is observed with Cryo-TEM at high magnification (Fig. S4). The

339 decreases in MSR and aggregate zeta potential for SDBS as  $C_w$  goes above CMC are  
340 probably a result of micelle formation. At surfactant concentrations higher than  
341 CMC, a new partitioning equilibrium of surfactant between the bulk solution,  
342 hexadecane/water interface, and micelles is established. In this case,  $C_w$  remains at  
343 CMC and is insensitive to the change of  $C_0$ , and so are  $\Gamma$  and  $d$ . Hence, the regime of  
344 HOCs solubilization by surfactants at concentrations above CMC differs from that  
345 below CMC.

346

## 347 **5. Conclusion**

348 In contrast to the conceptualized micelle-based mechanism for solubilization of  
349 HOCs starting at surfactant concentration higher than CMC, the results of this study  
350 demonstrated that SDBS and Triton X-100 at sub-CMC concentrations can enhance  
351 hexadecane solubilization employing an aggregate formation mechanism.  
352 Observation of sub-CMC aggregates by both DLS and cryo-TEM methods suggests  
353 that HOC-surfactant interaction contributes to sub-CMC aggregate formation, which  
354 is in contrast to pure-surfactant micelles formation above CMC. This is for the first  
355 time the sub-CMC solubilization of HOCs by surfactants is comprehensively  
356 explored. The study is of importance for better understanding the solubilization  
357 behavior of HOCs by surfactants and for economical application of surfactants.  
358 Future studies should aim at testing such sub-CMC solubilization behavior for a  
359 variety of surfactants and HOCs.

360

361 **Acknowledgments**

362 The authors thank the Center for Integrative Imaging (CII) at University of  
363 Science and Technology of China for cryo-TEM analysis. This study was funded by  
364 the National Student Innovation Training Program (SIT) of China (521611246), the  
365 National Natural Science Foundation of China (51378192, 51378190, 51308200 and  
366 51108166), the Program for Changjiang Scholars and Innovative Research Team in  
367 University (IRT-13R17). Additional support was provided by the NIEHS Superfund  
368 Research Program (ES04940).

369

370 **References**

- 371 1 L. M. Abriola, C. D. Drummond, E. J. Hahn, K. F. Hayes, T. C. G. Kibbey, L. D.  
372 Lemke, K. D. Pennell, E. A. Petrovskis, C. A. Ramsburg and K. M. Rathfelder,  
373 *Environ. Sci. Technol.*, 2005, **39**, 1778-1790.
- 374 2 J. Childs, E. Acosta, M. D. Annable, M. C. Brooks, C. G. Enfield, J. H. Harwell,  
375 M. Hasegawa, R. C. Knox, P. S. Rao, D. A. Sabatini, B. Shiau, E. Szekeres and  
376 A. L. Wood, *J. Contam. Hydrol.*, 2006, **82**, 1-22.
- 377 3 R. Masrat, M. Maswal and A. A. Dar, *J. Hazard. Mater.*, 2013, **244**, 662-670.
- 378 4 K. D. Pennell, L. M. Abriola and W. J. Weber Jr, *Environ. Sci. Technol.*, 1993, **27**,  
379 2332-2340.
- 380 5 D. E. Kile and C. T. Chiou, *Environ. Sci. Technol.*, 1989, **23**, 832-838.

- 381 6 Y. Zhang and R. M. Miller, *Appl. Environ. Microb.*, 1992, **58**, 3276-3282.
- 382 7 J. E. McCray, G. Bai, R. M. Maier and M. L. Brusseau, *J. Contam. Hydrol.*,  
383 2001, **48**, 45-68.
- 384 8 S. Peng and M. L. Brusseau, *Water Resour. Res.*, 2005, **41**, 6874-6880.
- 385 9 J. S. Clifford, M. A. Ioannidis and R. L. Legge, *J. Colloid Interface Sci.*, 2007,  
386 **305**, 361-365.
- 387 10 J. D. Albino and I. M. Nambi, *J. Environ. Sci. Heal. A*, 2009, **44**, 1565-1573.
- 388 11 A. Patist, J. R. Kanicky, P. K. Shukla and D. O. Shah, *J. Colloid Interface Sci.*,  
389 2002, **245**, 1-15.
- 390 12 M. A. Mir, O. A. Chat, M. H. Najjar, M. Younis, A. A. Dar and G. M. Rather, *J.*  
391 *Colloid Interface Sci.*, 2011, **364**, 163-169.
- 392 13 A. R. Tehrani-Bagha and K. Holmberg, *Materials*, 2013, **6**, 580-608.
- 393 14 H. Zhong, Y. Liu, Z. F. Liu, Y. B. Jiang, F. Tan, G. M. Zeng, X. Z. Yuan, M. Yan,  
394 Q. Y. Niu and Y. S. Liang, *Int. Biodeter. Biodegr.*, 2014, **94**, 152-159.
- 395 15 U. Zoller, *Environ. Int.*, 2006, **32**, 269-272.
- 396 16 S. S. Talmage, *Environmental and human safety of major surfactants: alcohol*  
397 *ethoxylates and alkylphenol ethoxylates*, CRC Press, 1994.
- 398 17 S. Rebello, A. K. Asok, S. Mundayoor and M. Jisha, *Environmental chemistry*  
399 *letters*, 2014, **12**, 275-287.
- 400 18 K. Hill and C. LeHen-Ferrenbach, in *Sugar-based surfactants fundamentals and*  
401 *Applications*, ed. C. C. Ruiz, CRC Press, Boca Raton, 2008.



- 402 19 R. Höfer and K. Hinrichs, in *Polymers-Opportunities and Risks II: Sustainability,*  
403 *Product Design and Processing*, Springer, Berlin, Heidelberg, 2010, pp. 97-145.
- 404 20 K. Hill and R. Höfer, in *Sustainable Solutions for Modern Economies*, ed. R.  
405 Höfer, RSC Publishing, Cambridge, 2009, pp. 167-237.
- 406 21 L. Chen and T. C. Kibbey, *Langmuir*, 2006, **22**, 6874-6880.
- 407 22 M. J. Rosen, *Surfactants and Interfacial Phenomena*, John Wiley & Sons,  
408 Hoboken, 3rd edn., 2004.
- 409 23 X. Z. Yuan, F. Y. Ren, G. M. Zeng, H. Zhong, H. Y. Fu, J. Liu and X. M. Xu,  
410 *Appl. Microbiol. Biot.*, 2007, **76**, 1189-1198.
- 411 24 R. J. Zasoski, in *Encyclopedia of Soil Science*, ed. W. Chesworth, Springer  
412 Netherlands, Dordrecht, 2008, pp. 841-845.
- 413 25 H. Zhong, G. M. Zeng, J. X. Liu, X. M. Xu, X. Z. Yuan, H. Y. Fu, G. H. Huang,  
414 Z. F. Liu and Y. Ding, *Appl. Microbiol. Biot.*, 2008, **79**, 671-677.
- 415 26 K. Yang, L. Zhu and B. Xing, *Environ. Sci. Technol.*, 2006, **40**, 4274-4280.
- 416 27 Sigma-Aldrich, Selected properties of Triton X-100, [http://www.sigmaaldrich](http://www.sigmaaldrich.com/catalog/product/sial/x100?lang=zh&region=CN)  
417 [h.com/catalog/product/sial/x100?lang=zh&region=CN](http://www.sigmaaldrich.com/catalog/product/sial/x100?lang=zh&region=CN) [In Chinese], (accessed  
418 April 8, 2015).
- 419 28 D. A. Edwards, R. G. Luthy and Z. Liu, *Environ. Sci. Technol.*, 1991, **25**,  
420 127-133.
- 421 29 I. B. Ivanov, K. G. Marinova, K. D. Danov, D. Dimitrova, K. P.  
422 Ananthapadmanabhan and A. Lips, *Adv. Colloid Interface Sci.*, 2007, **134**,

- 423 105-124.
- 424 30 D. Q. Lin, L. N. Zhong and S. J. Yao, *Biotechnol. Bioeng.*, 2006, **95**, 185-191.
- 425 31 W. Liu, J. Kumar, S. Tripathy and L. A. Samuelson, *Langmuir*, 2002, **18**,
- 426 9696-9704.
- 427 32 NCBI, PubChem Compound Database; CID=11006, selected properties of
- 428 n-Hexadecane, <http://pubchem.ncbi.nlm.nih.gov/compound/11006>, (accessed
- 429 May 8, 2015).
- 430 33 J. Penfold, I. Tucker, R. Thomas, E. Staples and R. Schuermann, *J. Phys. Chem.*
- 431 *B*, 2005, **109**, 10760-10770.
- 432 34 D. A. Dzombak and F. M. M. Morel, *Surface Complex Modeling, Hydrous Ferric*
- 433 *Oxide*, John Wiley & Sons, New York, 1990.
- 434 35 R. J. Hunter, *Zeta Potential in Colloid Science. Principles and Applications*,
- 435 Academic Press, New York, 1981.
- 436 36 G. Bai, M. L. Brusseau and R. M. Miller, *J. Contam. Hydrol.*, 1998, **30**,
- 437 265-279.
- 438 37 C. L. Chun, J.-J. Lee and J.-W. Park, *Environ. Pollut.*, 2002, **118**, 307-313.
- 439 38 S. Paria, *Adv. Colloid Interface Sci.*, 2008, **138**, 24-58.
- 440

**Table 1** Selected properties and the water-hexadecane interface coefficients of the surfactants used in this study

<i>Surfactant</i>	<i>Formula</i>	<i>Surfactant type</i>	<i>Molecular weight (g/mol)</i>	<i>CMC<sup>a</sup> (μM)</i>	<i>Γ<sub>max</sub><sup>b</sup> (mol/m<sup>2</sup>)</i>	<i>A<sub>m</sub><sup>c</sup> (nm<sup>2</sup>)</i>	<i>K<sup>d</sup> (m<sup>3</sup>/mol)</i>
SDBS	C <sub>12</sub> H <sub>25</sub> C <sub>6</sub> H <sub>4</sub> SO <sub>3</sub> Na	Anionic	348.48	612	3.3 × 10 <sup>-6</sup>	0.50	0.2 × 10 <sup>3</sup>
Triton X-100	C <sub>8</sub> H <sub>17</sub> C <sub>6</sub> H <sub>4</sub> O(CH <sub>2</sub> CH <sub>2</sub> O) <sub>10</sub> H	Non-ionic	648.86	672	1.9 × 10 <sup>-6</sup>	0.87	4.3 × 10 <sup>3</sup>

<sup>a</sup> Critical micelle concentration (CMC) measured in PBS solution at 30 °C

<sup>b</sup> Maximum interface excess of surfactant

<sup>c</sup> Area per surfactant molecule at Γ<sub>max</sub>.

<sup>d</sup> Langmuir equation constant

**Figure 1** The molecular structure of SDBS and Triton X-100.

**Figure 2** (a) The hexadecane/PBS interfacial tension as a function of surfactant concentration. (b) Interfacial tension-concentration relation regression at surfactant concentrations below CMCs using Szyszkowski equation (Equation (3) in text).

**Figure 3** Apparent hexadecane solubility ( $C_{\text{hex}}$ ) versus total surfactant concentration ( $C_0$ ) of (a) SDBS and (b) Triton X-100. Two sets of regression represent data for below and above the CMCs.

**Figure 4** Aggregate size ( $d$ ) versus the total surfactant concentration ( $C_0$ ) for hexadecane solubilization. (Insert) Zoom-in for  $C_0$  lower than CMC.

**Figure 5** Zeta potential of aggregates versus the total surfactant concentration ( $C_0$ ) for the hexadecane solubilization.

**Figure 6** (a) Apparent solubility of hexadecane ( $C_{\text{hex}}$ ) versus the bulk surfactant concentration ( $C_w$ ) at  $C_w$  below CMCs; (b) surface excess ( $\Gamma$ ) and molecule area ( $A$ ) of surfactants on the aggregates surface versus surfactant bulk concentration ( $C_w$ ). The dash lines and dash dot lines represent the maximum surface excess ( $\Gamma_{\text{max}}$ ) and the minimum area per surfactant molecular on the surface ( $A_m$ ), respectively.

**Figure 7** Aggregates diameter ( $d$ ) and surface excess of surfactants ( $\Gamma$ ) versus the bulk surfactant concentration ( $C_w$ ) below CMCs.

**Figure 8** Schematic diagram of aggregate formation at surfactant concentration below CMCs and the change of curvature of aggregates surface with increasing surfactant bulk concentration for the hexadecane solubilization by surfactant.

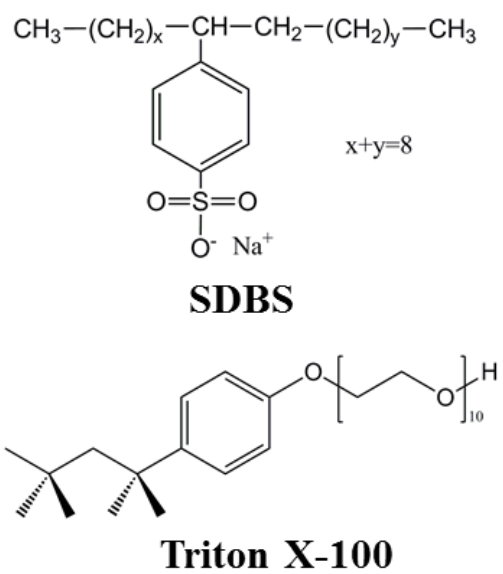


Figure 1

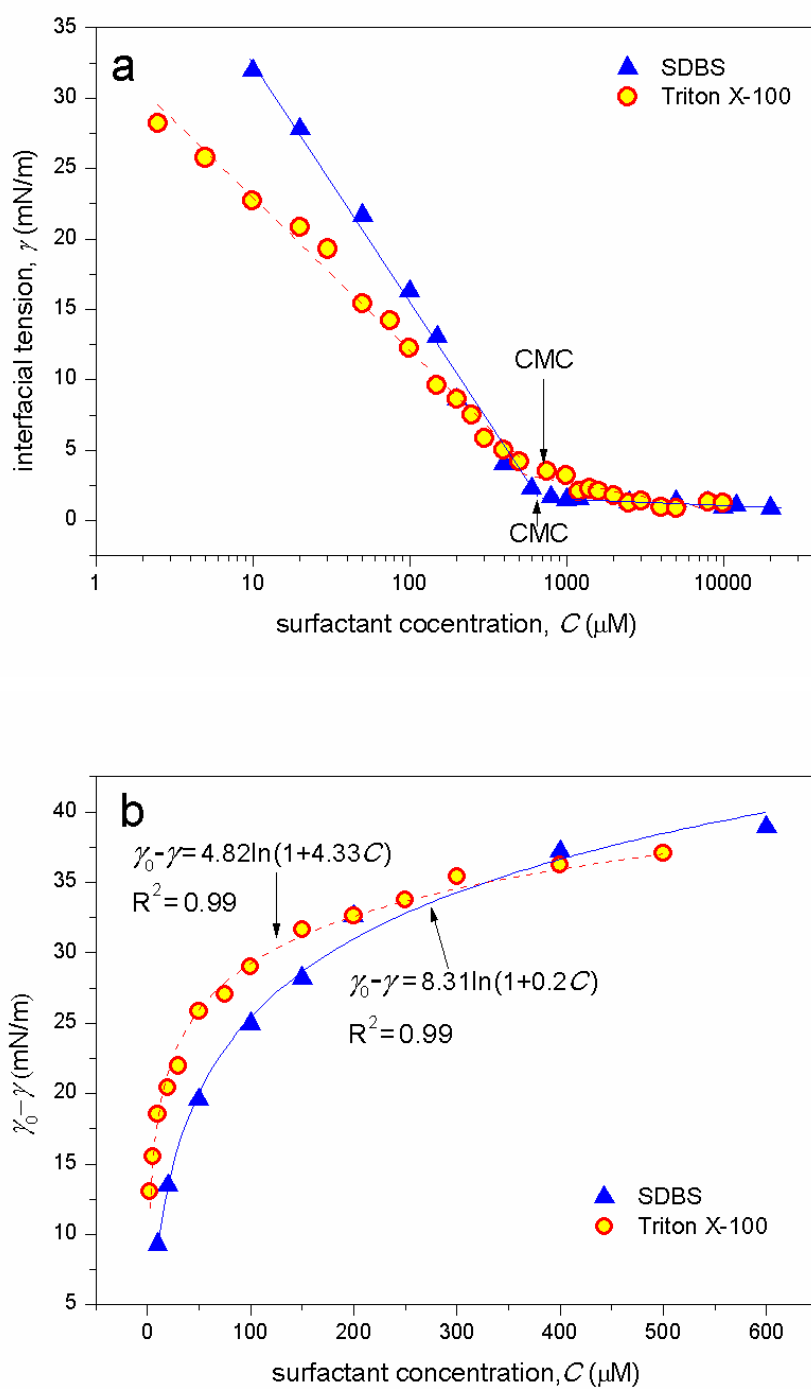


Figure 2

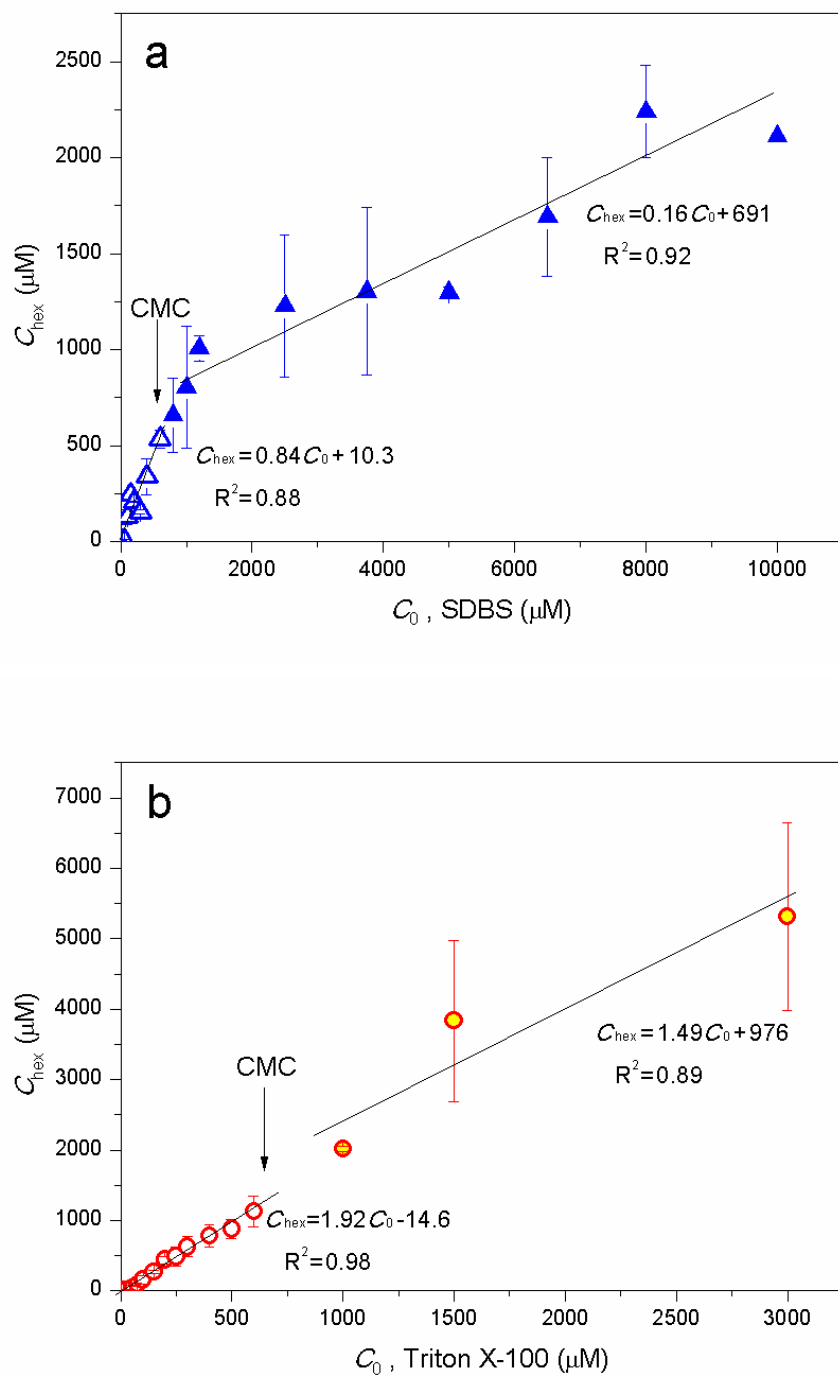


Figure 3



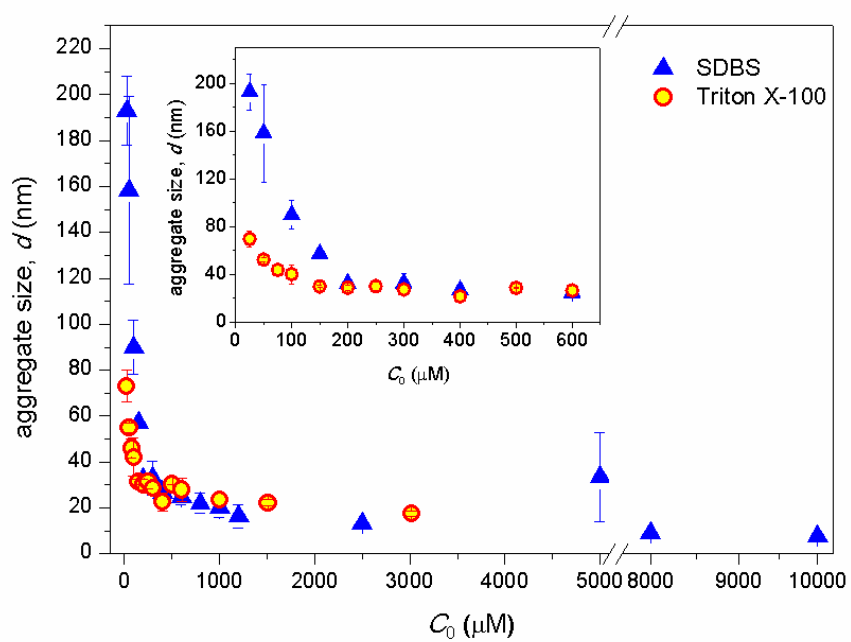


Figure 4

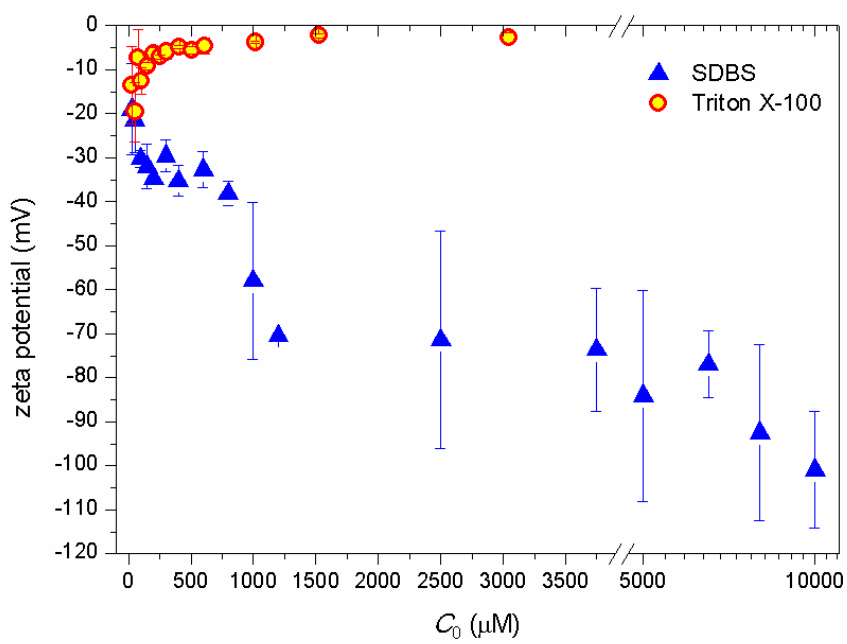


Figure 5

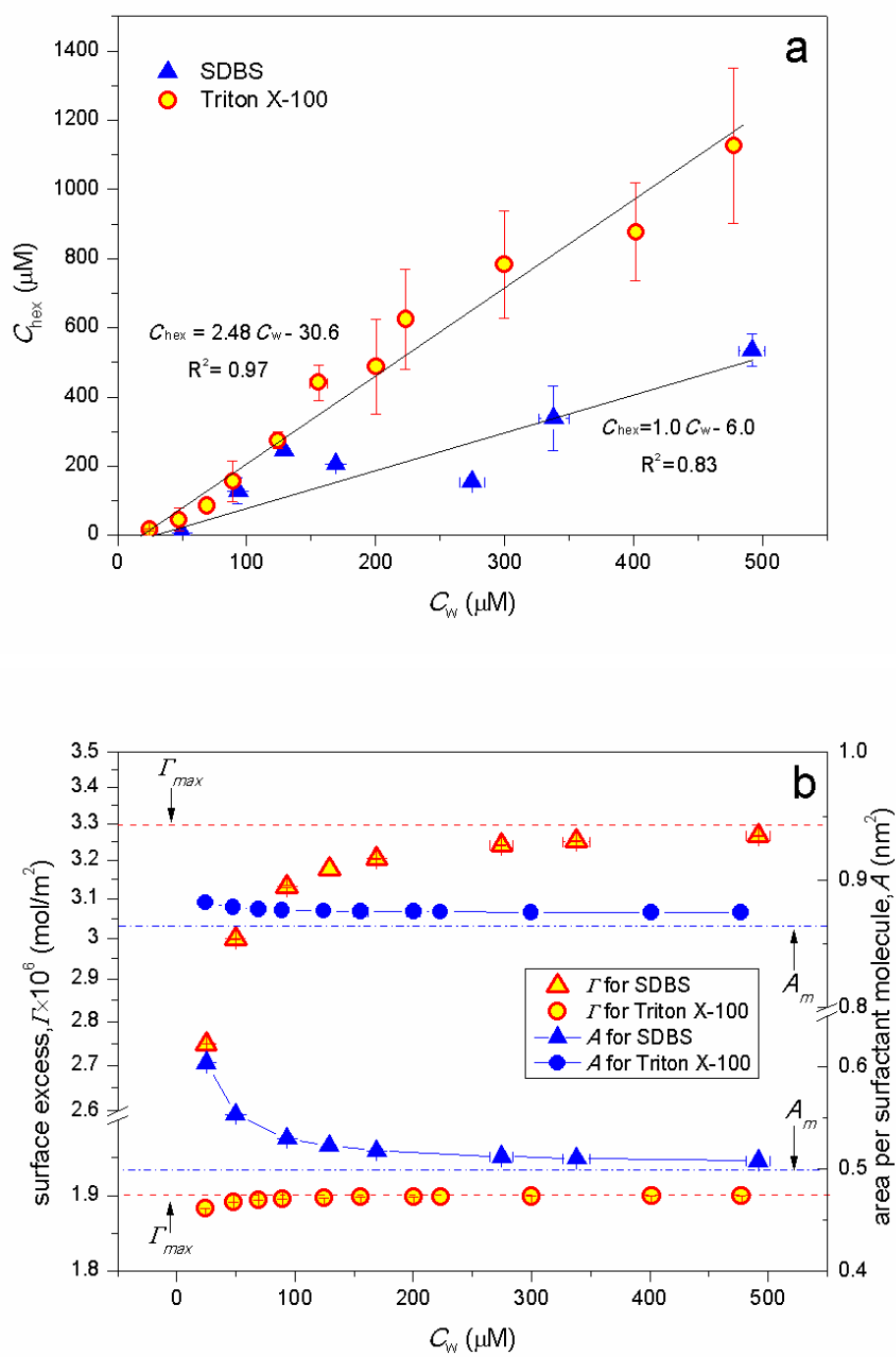


Figure 6

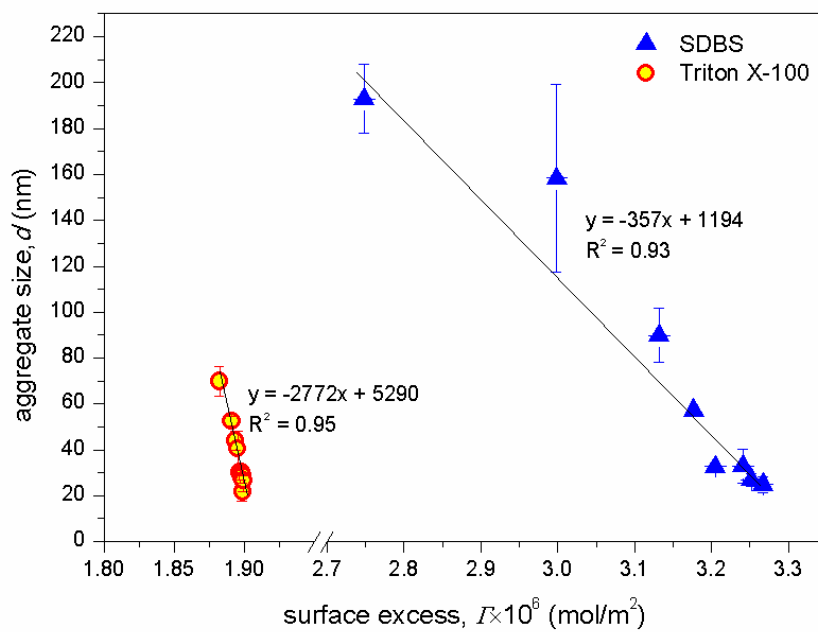


Figure 7

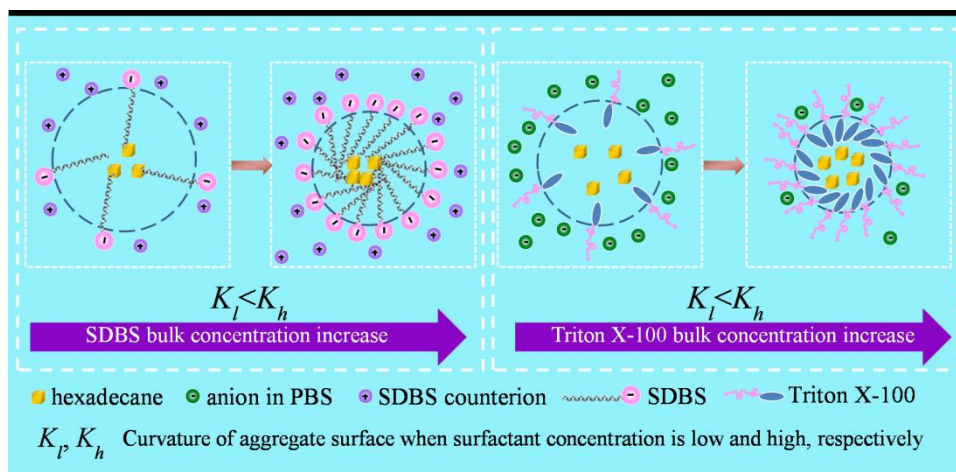


Figure 8